

Available online at www.sciencedirect.com**ScienceDirect**

Procedia Technology 24 (2016) 477 – 484

Procedia
TechnologyInternational Conference on Emerging Trends in Engineering, Science and Technology (ICETEST
- 2015)

Mathematical Model for a Novel Cryogenic Flow Sensor using Fibre Bragg Gratings

S. R. Thekkethil^{a,b}, K. E. Reby Roy^b, R. J. Thomas^b, H. Neumann^a, R. Ramalingam^{a*}^a*Institute for Technical Physics, Karlsruhe Institute of Technology, Germany*^b*Dept. of Mechanical Engineering, T. K. M. College of Engineering, Kollam, India*

Abstract

In this work, a mathematical model is presented for a newly developed cryogenic flow meter which is based on fibre Bragg grating (FBG) principle. The principle of operation is to use the viscous drag force induced by a flowing fluid on an optical fibre placed transverse to the flow. An optical fibre will have a 5 mm long grating element inscribed in it and will be placed so that the sensor is at the centre of the pipe. The fibre will act as the bluff body, while the FBG sensor will pick up the bending strain induced in the fibre due to the drag force. The amount of bending strain which can be measured as a shift in Bragg wavelength can be calibrated to provide the mass flow rate. Here a mathematical model is being presented to predict the operation of the sensor and to calculate the sensor characteristics so that the sensor design can be optimised. The sensor exhibits an exponential relationship between sensitivity and mass flow rate. It is also seen that the sensitivity depends greatly on the fluid properties such as density and viscosity.

© 2016 The Authors. Published by Elsevier Ltd. This is an open access article under the CC BY-NC-ND license (<http://creativecommons.org/licenses/by-nc-nd/4.0/>).

Peer-review under responsibility of the organizing committee of ICETEST – 2015

Keywords: Flow meter; Fibre Bragg gratings; Low temperature measurement; Sensors; Cryogenics

* Corresponding author. Tel.: +49-721-608-23827

E-mail address: rajini-kumar.ramalingam@kit.edu

1. Introduction

It is essential to understand the thermodynamic process and the cooling efficiency in most of the cryogenic and superconductor applications. The flow characteristics of coolant flowing in the cooling channels can give the thermos physical behaviour of the system. Hence the accurate measurement of fluid flow characteristics plays prominent role in any machinery that comprises a fluid flow or convection heat transfer. It is preferable to have a flow measurement which does not affect the flow characteristic during the measurement. The mounted meter, ideally should not induce a pressure drop or change the temperature of the flow. The brittle behaviour of materials at low temperatures and the thermal stresses due to large changes in temperature restrict the use of many existing designs and materials for these applications. The pressure drops due to the introduction of the measurement device also pose a serious concern in cryogenic flows. The chances of cavitation are quite high in case of cryogenes, since the temperature of flow is very near to its saturation temperature. This makes mass flow meters based on differential pressure, such as laminar flow meters or orifice meters a bad solution for such applications. Additionally, the new applications like high temperature superconducting generators which rotate at 3000 rpm, which is cooled small diameter tubes.

There are other intrinsic difficulties associated with the use of traditional sensor technologies in superconductors and space applications. The absence of gravity restricts use of many flow measuring methods such as rotameters. The high electromagnetic fields present in superconductors will introduce errors in the commonly used electronic flow meters. Other requirements for such applications include small size, remote sensing capabilities, replicability, long life etc.

Nomenclature

λ_b	Bragg wavelength
Δ	Grating period
η_{eff}	Effective refractive index
$\Delta\lambda_b$	Bragg shift
\dot{m}	Mass flow rate
ρ	Density of fluid
A	Cross sectional area
F_d	Drag force
C_d	Drag coefficient
A_p	Projected area
d_f	Diameter of fibre
L	Length of fibre
E_{eff}	Effective Young's modulus
P_e	Strain-optic coefficient
P_{11}, P_{12}	Components of strain-optic tensor
n	Refractive index
ν	Poisson's ratio
α	Thermal expansion coefficient
ξ	Thermo-optic coefficient

The above problems could be solved by using an optical based FBG measurement system. FBG has been recently getting more popular in cryogenic and superconductor fields for different applications (Jicheng Li et. al., 2015).

1.1. Fibre Bragg Grating Sensors

A fibre Bragg grating (FBG) is an optical filter embedded in an optical fibre, by means of placing a set of gratings at specified distances. A grating is an area of altered refractive index, placed in a homogeneous domain.

A FBG sensor is introduced in an optical fibre by using high power UV laser. Two UV laser beams are allowed to intersect at a specific angle on an optical fibre. The constructive and destructive interference of the UV will alter the bonding of doping elements in the fibre creating areas of varying refractive indices. The distance between the gratings can be fixed by fixing the wavelength of the UV laser and the angle of incidence (θ) (Fig. 1).

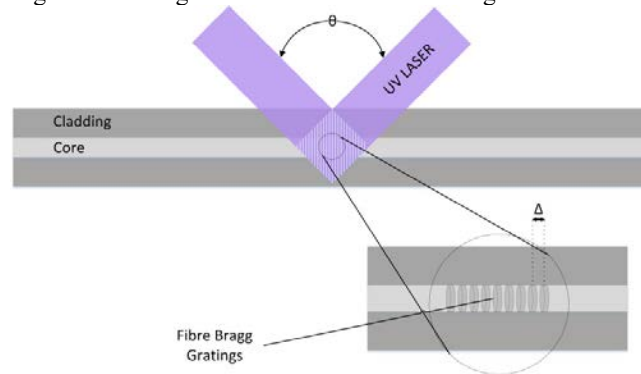


Fig. 1 Schematic of fabrication of FBG sensor

The operation of a FBG sensor can be explained as a filter. When a beam of white light, i.e. light with full spectrum, is passed into a FBG sensor, the sensor reflects light of a specific wavelength while allowing all other wavelengths to pass through without distortion (Fig. 2). In case of multiple sensors placed in a single fibre (multiplexing), the reflected wavelength can be selected so that each FBG sensor has a distinct operational range.

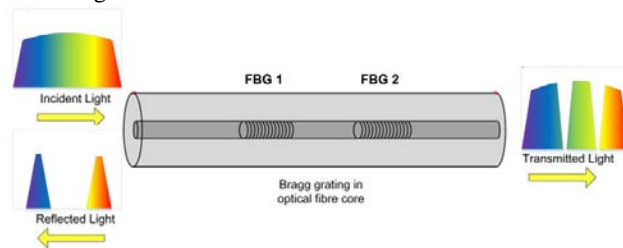


Fig. 2 Operation of a FBG sensor

The single wavelength that is reflected by an FBG sensor is called the Bragg wavelength and is dependent on the grating period (Δ). The Bragg wavelength is correlated in Byoungho Lee, 2003 as

$$\lambda_b = 2\Delta n_{eff} \quad (1)$$

When strain is applied on a FBG sensor, the distance between the gratings (grating period) changes. This will attribute as a change in the reflected wavelength as defined by Eqn. 1. This change in the reflected wavelength is called Bragg shift ($\Delta\lambda_b$).

This property of an FBG sensor to measure very large strains (up to 5000 $\mu\text{m}/\text{m}$) with good accuracy has enabled its use in measurement of various physical parameters such as displacement, temperature, pressure, strain, vibration, acceleration, velocity, torsion, fluid flow etc. The inherent properties of a FBG sensor and use of optical fibre also deliver various advantages such as remote sensing, passive operation, corrosion resistance, multiplexing capabilities of up to 10 FBG sensors in a single optical fibre by using wavelength division multiplexing (WDM), small size (150 μm dia), measurement of multiple parameters using a single fibre, imperviousness to electrical & magnetic interference, long distance signal transfer without repeaters etc.

1.2. FBG as a flow sensor

Numerous independent researches have been conducted worldwide on the use of FBG sensors as a flow meter. A large numbers of studies were concentrated on the use of FBG sensors in flow measurement by using the principle of anemometry. A laser beam was used to heat the FBG sensor to a stable temperature. The flowing fluid will carry away a part of heat reducing the temperature. The change in temperature which can be sensed by the FBG sensor itself will give an indication of the flow rate. Such a concept was introduced by Xinhui Wang, et. al., 2014. A different approach was introduced in J. H. Shim et. al., 2008, which was to use FBG for temperature measurement of fluid downstream to a heating coil. The temperature of downstream fluid will be according to the flow rate. These approaches showed minimum pressure drop but were not applicable in many cases due to the heat addition to the flow. These devices were predominantly fluids at atmospheric conditions and were not pertinent for cryogenic liquids. The introduction of heat in to the system is not preferred in case of cryogenic flows.

A different conception explored by various researchers was the use of FBG sensors in target type flow meters (Xueguang Qiao et. al., 2008). In this concept, a target body is placed in the fluid. The impact of fluid on the target will create a stress on the support structure. This stress can be measured using FBG sensors. Though this concept was theoretically applicable for cryogenic fluids, the pressure drop across the sensor was usually high. An innovative concept was presented in R. Ramalingam et. al., 2013, where instead of the impact force, the drag force due to the fluid flow was used to movement of a target. Here the target was designed to be a cylinder placed close to the pipe walls. Thus this design eliminated the problem of pressure drop. Few studies were conducted in this direction showing promising results.

2. Single fibre flowmeter

In this design, the concept of using a discrete target body is eliminated. Instead the FBG fibre is placed directly in the path of flow, such that the fibre is perpendicular to the direction of flow. The viscous drag created due to the flow will cause a bending force on the on the fibre.

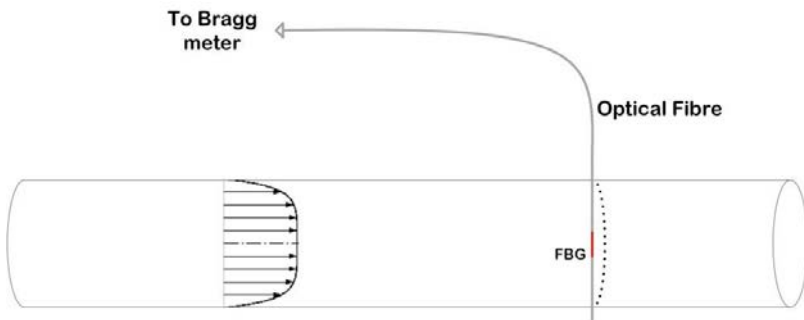


Fig. 3 Operation of FBG based flow meter

2.1. Operation Principle

The operating principle of this design is the viscous drag created by a fluid when flowing past a bluff body is proportional to its velocity or mass flow rate. The mass flow rate (\dot{m}) can be related to the flow velocity (v) as

$$\dot{m} = v \cdot \rho \cdot A \quad (2)$$

Based on this, the drag force (F_d) due to the flow can be calculated by substituting the mass flow rate in the drag equation as

$$F_d = 0.5 C_d \cdot A_p \cdot \dot{m}^2 / (\rho \cdot A^2) \quad (3)$$

where C_d , the drag coefficient, is estimated as 1.1 for a cylinder placed perpendicular to flow. The projected area of the fibre, A_p can be expressed in terms of the fibre diameter (d_f) and fibre length (L) as

$$A_p = d_f * L \quad (4)$$

Beam theory is applied to find the bending strain induced in the fibre. The FBG fibre may be assumed to be a fixed beam, since both the ends are clamped in the vacuum tight seal. The drag force can be assumed to be an Uniformly Distributed Load (UDL) acting on it. With that assumption, the total strain on the FBG sensor may be given by the equation,

$$\varepsilon = F_d * L / (3 * 0.78 * d_f^3 * E_{eff}) \quad (5)$$

The response of a FBG sensor for the given value of mechanical strain in terms of Bragg wavelength shift can be evaluated as (A. Othonos, 1997)

$$\Delta\lambda_{b1} = (1 - P_e) * \varepsilon * \lambda_b \quad (6)$$

in which P_e is the effective strain-optic coefficient of the fibre, which is given as follows

$$P_e = 0.5 * n^2 * [P_{12} - \nu(P_{11} + P_{12})] \quad (7)$$

For a typical FBG sensor there values can be estimated as $P_{11} = 0.113$, $P_{12} = 0.252$, $\nu = 0.16$ and $n = 1.482$. For a FBG sensor with Bragg wavelength 1550 nm, the expected strain sensitivity can be found out as 1.2 pm for an applied strain of 1 $\mu\text{m}/\text{m}$.

The FBG sensor is further sensitive to temperature changes in its surroundings. This is due to the thermal strain created in the optical fibre. The Bragg wavelength shift due to change in temperature ($\Delta\lambda_{b2}$) is explained in V. N. Venkatesan et. al., 2015 and can be expressed as a function of change in temperature, ΔT as

$$\Delta\lambda_{b2} = (\alpha + \zeta) \Delta T \quad (8)$$

The thermal expansion coefficient and the thermo-optic coefficient for a germanium doped silica fibre are 0.55×10^{-6} and 8.6×10^{-6} respectively. The expected sensitivity for a fibre Bragg grating at 1550 nm is approximately 13.7 pm/K.

Based on these two independent factors that induce a strain, the total Bragg shift ($\Delta\lambda_b$) can be expressed as the sum of individual shifts.

$$\Delta\lambda_b = \Delta\lambda_{b1} + \Delta\lambda_{b2} \quad (9)$$

This property is quite significant during the use of FBG sensors, since the sensor used for strain measurement will automatically measure the temperature changes also. Due to this, while conducting measurements, a second FBG sensor must be used such a way that it only measures the temperature changes and thus can be used as a thermal compensator.

2.2. Sensor Design

In this work, the flow sensor was designed for a pipe of $\text{Ø}18$ mm. An operational range of 0-30 g/s was decided for the testing of gases. From Eqn. 3 it is evident that for a given mass flow rate, the drag force experienced by a bluff body placed in a fluid flow is inversely proportional to the density of fluid. Three different conditions were under consideration, which are atmospheric temperature, saturated gas and saturated liquid. Based on these parameters, as presented in R. A. Haefler, 1981, the maximum Reynold's number was calculated for different fluids.

When testing nitrogen gas or air, which are having a low viscosities, error due to vortex induced vibrations are expected in the measurements. Helium Gas and liquid cryogenics being more viscous are will dampen the vibrations giving a better output signal.

It was also verified that for the given range of operation, compressible flow does not occur, which can lead to pressure waves in the fluid domain. The drag force was calculated for the gases and cryogenic fluids under consideration, for their respective range of mas flow rates using the Eqn. 3. The results are shown in Fig. 4, Fig. 5.

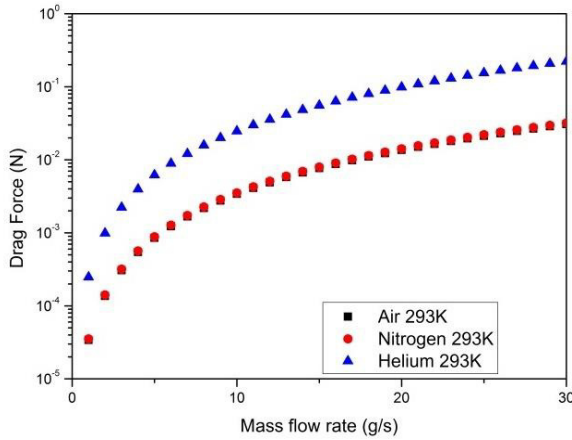


Fig. 4 Drag force (F_d) vs mass flow rate (\dot{m}) at atmospheric conditions

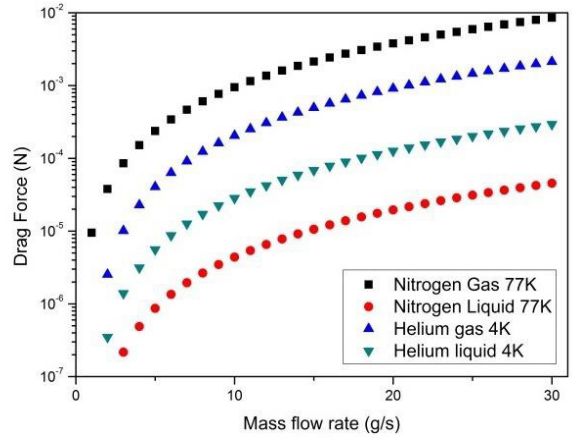


Fig. 5 Drag force (F_d) vs mass flow rate (\dot{m}) at cryogenic temperatures

Based on these values of drag force, the strain on fibre was calculated considering the FBG fibre as a fixed beam, on which the drag force is acting as a Uniformly Distributed Load (UDL). Equation 5 can be used to determine the strain in the fibre.

The effective Young’s modulus (E_{eff}) required for the calculation is estimated using the equation

$$d_f^2 * E_{eff} = (d_f^2 - d_c^2) E_f + d_c^2 * E_c \tag{10}$$

where subscripts ‘f’ and ‘c’ denotes the cladding and core respectively. Taking the values from Table 1, the Young’s modulus (E_{eff}) can be calculated to be 2.65×10^9 Pa.

Table 1 Design parametrs of core and cladding

	Diameter (m)	Young’s modulus (Pa)
Core	9×10^{-6}	7.33×10^{10}
Cladding	2×10^{-4}	2.50×10^9

Proportional to the values of stain developed in the fibre, the FBG sensor will exhibit a shift in wavelength ($\Delta\lambda_b$), which is governed by Eqn. 6. The wavelength shifts for different fluids were plotted and the response of the sensor was studied based on these values. It was seen that the output of the FBG sensor shows large variations for different fluids at the same mass flow rate. This is due to the large variations in density and viscosity of the fluids with respect to temperature.

3. Performance Study

The response and the performance parameters of the FBG sensor were predicted based on the theoretical studies.

3.1. Gases at Atmospheric Temperature

Helium, nitrogen and air at atmospheric temperature (293 K) were considered for this study. Among these, both air and nitrogen showed very similar response which is as expected. Helium showed a maximum shift of 86735 pm for a flow rate of 30 g/s, while nitrogen and air showed a Bragg shift of 12375 pm and 11971 pm respectively. Nitrogen showed a sensitivity of 151.2 pm/(g/s) at low flow rates (0-10 g/s) and a sensitivity of 701.3 pm/(g/s) at

high flow rates (21-30 g/s). The respective values for air were 146.32 pm/(g/s) and 678.37 pm/(g/s). Helium on the other hand showed a much higher sensitivity with 1060.1 pm/(g/s) at low flow rates and 4915 pm/(g/s) at higher flowrates. The average sensitivities over the whole range was ~360 pm/(g/s) for air and nitrogen while ~2500 pm/(g/s) for helium. Assuming the error during measurement to be ±2 pm, the resolution of the sensor may be calculated as ~0.5 g/s for nitrogen or air and ~0.2 g/s for helium.

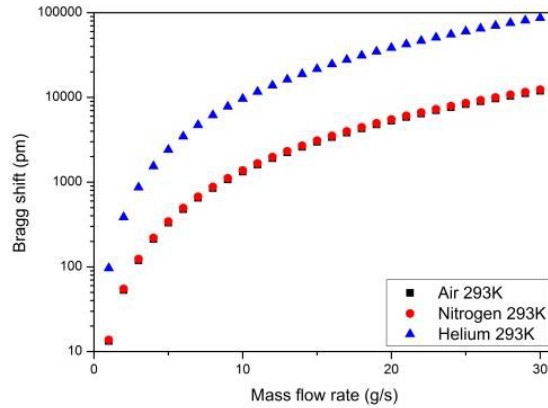


Fig. 6 Bragg shift ($\Delta\lambda_b$) vs mass flow rate (\dot{m}) for gases at atmospheric temperature (293 K)

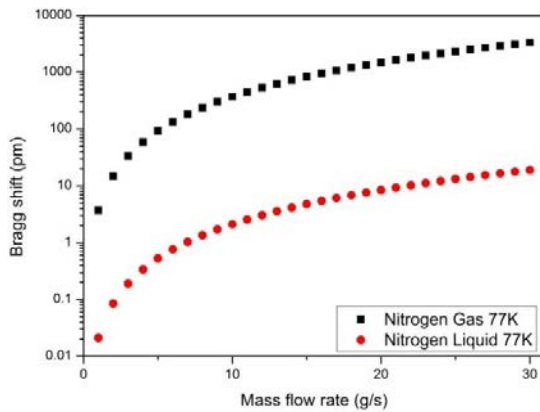


Fig. 7 Bragg shift ($\Delta\lambda_b$) vs mass flow rate (\dot{m}) for nitrogen

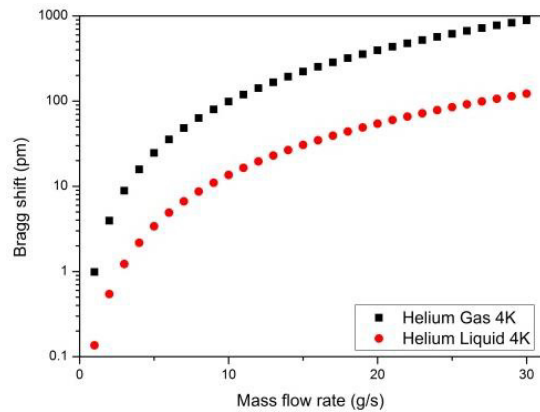


Fig. 8 Bragg shift ($\Delta\lambda_b$) vs mass flow rate (\dot{m}) for helium

3.2. Gases at Saturation Temperatures

At their saturation temperatures due to the low viscosities of the gases the flow velocities will be lower than that of the same gas at room temperature and same mass flow rate. This in turn can reduce the drag force and lead to low sensitivities. At their saturation temperatures, Helium showed a maximum Bragg shift of 888 pm at 30 g/s whereas nitrogen showed a 3327.7 pm. At low velocities, the sensor sensitivity was calculated to be 40.67 pm/(g/s) for nitrogen and 10.85pm/(g/s) for helium. At higher velocities, the sensitivities increased to 188.56 and 50.321 pm/(g/s) for nitrogen and helium respectively.

The overall sensitivity of nitrogen and helium over the whole range was 96.1 and 25.65 pm/(g/s). Further studies and experimental verification is required before understanding the feasibility of the sensor at this range. Further changes in the sensor design such as the pipe diameter etc. can aid in attaining a higher sensitivity. Due to the lower sensitivity, the sensor resolution was ~2 g/s for nitrogen and ~4 g/s for helium.

3.3. Cryogenic Liquids

Cryogenic liquid due to very high densities, need only a very small velocity to provide a good mass flow rate. The performance of the sensor while using cryogenic liquids were tested in a range of 0-30g/s. This provided a lower velocity range which is reflected in the response of the sensor.

For liquid nitrogen, at 30 g/s the fluid velocity was 0.18 m/s creating only a small shift of 18.9 pm in the Bragg wavelength. The low and high range sensitivities were calculated to be 0.23 and 1.07 pm/(g/s) for liquid nitrogen while 1.5 and 7 pm/(g/s) for liquid helium. Overall sensitivities of 0.65 and 4.2 pm/(g/s) were obtained for liquid nitrogen and liquid helium. The resolution of the instrument was calculated to be 15 g/s and 5 g/s for nitrogen and helium respectively.

4. Measurement of two-phase flow

It is evident from Fig. 7 and Fig. 8 the response of the FBG sensor towards the saturated liquid and saturated gas is fairly different. The Bragg shift in the corresponding cases varies by several orders of magnitude. In case of helium the Bragg shift reduces by an order of 10 when moving from gaseous state to liquid state. In nitrogen, it can be seen that the Bragg shift is decreasing by a factor of 100 at 30 g/s, when the fluid phase changes from gas to liquid. In both cases, this response can be used for the estimation of state of fluid flow in two phase, such as slug flow, mist flow etc. In case of a bubble present in a liquid domain, the FBG sensor will exhibit a sudden Bragg shift indicating the chances of a slug flow. The designed system can be thus be used for two phase flows. In case of nearly homogeneous flows, such as mist flow or bubble flow, by averaging over the response of two or more sensors places in near field, a very accurate measurement flow rate of the two phase flow can be done which is a rising requirement in many cryogenic applications.

5. Conclusions

An innovative notion to use the FBG sensor to measure the mass flow rate for fluids was conceptualised through this work. The proposed design can be used at atmospheric and cryogenic temperatures. It will be impervious to electromagnetic fields and will only induce a negligible pressure drop. It is also expected that the current design will operate well in the two phase region providing measurement of mixed flows also.

A mathematical model was presented in this work, and the performance characteristics of the sensor were studied and sensitivity and resolution of the sensor were calculated. Further validation of this theoretical model will be done by experimental studies.

References

- [1] Jicheng Li, H. Neumann, R. Ramalingam, 2015. Design, fabrication, and testing of fiber Bragg grating sensors for cryogenic long-range displacement measurement. *Cryogenics*, Volume 68, Pages 36-43, ISSN 0011-2275
- [2] ByoungHo Lee, 2003 .Review of the present status of optical fiber sensors. *Optical Fiber Technology*, Volume 9, Issue 2, Pages 57-79
- [3] Xinhuai Wang, Xinyong Dong, Yan Zhou, 2014. Optical Fiber Flowmeter Using Silver-coated FBG Cascaded by Waist-enlarged Bitaper. *Progress In Electromagnetics Research Symposium Proceedings, China*, 835-838
- [4] J. H. Shim, S. J. Cho, Y. H. Yu, K. R. Sohn, 2008. Gas-flow sensor using optical fibre Bragg grating (FBG). *Journal of Navigation and Port Research International Edition*, 32(9), 717-722, ISSN-1598-5725
- [5] Xueguang Qiao, Qian Zhang, Haiwei Fu, Dakuan Yu, 2008. Design of the target type flowmeter based on fiber Bragg grating and experiment. *Journal of Chinese Optics Letters*, 6(11): pp.815-817
- [6] R. Ramalingam, H. Neumann, M. Süsler, 2013. Mass flow sensor and method for determining the mass flow in a pipe. Patent Application Publication, US 20130014594 A1.
- [7] Othonos, 1997. Fiber Bragg gratings. *Review of Scientific Instruments*, 68, 4309-4341
- [8] V. N. Venkatesan; K-P. Weiss; R. Ramalingam; 2015. Strain Calibration of Substrate-Free FBG Sensors at Cryogenic Temperature. *International Conference on Sensor Systems and Software*, Rome, Italy
- [9] R. A. Haefer, 1981. *Kryo-Vakuumentchnik: Grundlagen und Anwendungen*. Springer-Verlag, Berlin, <https://www.itep.kit.edu/english/192.php>, dt. 15/09/2015.